DOI: 10.24996/ijs.2026.67.11.2

ISSN: 0067-2904

Eco-friendly Fabrication of Silver Nanoparticles Using Echinops spinosissimus Seeds Extract: Optimization, Characterization, Antibacterial Efficacy, and Nano- Induced Red Blood Cell Hemolysis

Shahad Fadhel Ali *, Wadhah Naji Jasim
Department of Chemistry, College of Science, University of Baghdad, Baghdad, Iraq

Received: 29/6/2025 Accepted: 15/2/2026 Published: xx

ABSTRACT

The silver nanoparticles (AgNPs) were synthesized in aqueous media by means of an aqueous extract from Echinops spinosissimus seeds, and the optimization of the synthesis conditions was carried out at: 10 mL of extract + 10 mL of $AgNO_3$ (0.02 M), pH = 7, T = 70 °C during 60 minutes. The characterization of the product was performed through techniques such as UV-Vis spectroscopy, infrared spectroscopy, X-ray diffraction and scanning electron microscopy. The UV-Vis spectroscopy spectra showed a surface plasmonic resonance band characteristic of the metallic core of the nanomaterials; the FTIR data provided evidence of the presence of phytochemical molecules capping the AgNPs; finally, the SEM micrographs showed that the majority of the synthesized AgNPs had a spherical morphology, while some of them exhibited a rod-like shape (diameter range 46.69–71.99 nm). To evaluate the antimicrobial potential of the AgNPs synthesized, agar diffusion assays were conducted against three strains of bacteria (Escherichia coli, Klebsiella spp., Staphylococcus aureus) and two strains of fungi (Candida spp.). The results obtained from these assays showed a concentration-dependent inhibition of bacterial and fungal growth, and the mean diameters of the inhibition zones ranged approximately from 14–18 mm for both types of microorganisms tested. The hemocompatibility of the AgNPs was assessed using purified human red blood cells exposed to different doses of the synthesized AgNPs. A progressive increase in hemolysis was observed as a function of the increasing dose of AgNPs, which enabled to determine a "safe" window of application for the use of AgNPs as antimicrobial agents, balancing their efficacy against bacteria and fungi with their potential toxicity to humans.

Keywords: Silver Nanoparticles, Echinops spinosissimus, green synthesis, Hemolytic Activity

تصنيع صديق للبيئة لدقائق الفضة النانوية بأستخدام مستخلص بذور نبات شوك الجمل : تحسين العملية، ودراسة خصائصها، وفعاليتها المضادة للبكتيريا، وتأثيرها على تحلل خلايا الدم الحمراء

شهد فاضل علي*, وضاح ناجي جاسم
قسم الكيمياء, كلية العلوم, جامعة بغداد, بغداد, العراق

*Email: shahad.ali2305@sc.uobaghdad.edu.iq

Open Access Articles. This articles is licensed under CC BY

الخلاصة.

تم تصنيع جسيمات الفضة النانوية (AgNPs) في وسط مائي باستخدام مستخلص مائي من بذور نبات القرصعن الشائك(Echinops spinosissimus) ، وتم تحسين ظروف التصنيع عند: 10 مل من المستخلص + 10 مل من نترات الفضة (0.02 مولر)، ودرجة حموضة = 7، ودرجة حرارة = 70 درجة مئوية لمدة 60 دقيقة. أجريت توصيف المنتج باستخدام تقنيات مثل مطيافية الأشعة فوق البنفسجية–المرئية، ومطيافية الأشعة تحت الحمراء، وحيود الأشعة السينية، والمجهر الإلكتروني الماسح. أظهرت أطياف مطيافية الأشعة فوق البنفسجية–المرئية حالة رنين البلازما السطحية المميزة للب المعدني للمواد النانوية؛ قدمت بيانات مطيافية الأشعة تحت الحمراء بتحويل فوري دليلاً على وجود جزيئات كيميائية نباتية تغلف جسيمات الفضة النانوية؛ وأخيراً، أظهرت الصور المجهريّة الإلكترونية الماسحة أن غالبية جسيمات الفضة النانوية المصنعة كانت ذات مورفولوجيا كروية، بينما أظهرت بعضها شكلاً قضيبياً (مدى القطر 46.69–71.99 نانومتر). لتقييم القدرة المضادة للميكروبات لجسيمات الفضة النانوية المصنعة، أجريت اختبارات الانتشار في الأgarضد ثلاث سلالات من البكتيريا(Escherichia coli) ، Klebsiella spp.، Staphylococcus aureus)وسلالتين من الفطريات (Candida spp.).أظهرت النتائج المستحصلة من هذه الاختبارات تثبيطاً تركيزياً معتمداً لنمو البكتيريا والفطريات، وتراوحت متوسطات أقطار مناطق التثبيط تقريباً بين 14–18 ملم لكلا النوعين من الكائنات الدقيقة المختبرة. تم تقييم التوافق الدموي لجسيمات الفضة النانوية باستخدام خلايا الدم الحمراء البشرية المنقاة المعرضة لجرعات مختلفة من جسيمات الفضة النانوية المصنعة. لوحظ زيادة تدريجية في التحلل الدموي كدالة للجرعة المتزايدة من جسيمات الفضة النانوية، مما مكّن من تحديد نافذة "آمنة" للتطبيق لاستخدام جسيمات الفضة النانوية كعوامل مضادة للميكروبات، موازنةً بين فعاليتها ضد البكتيريا والفطريات وسميتها المحتملة للبشر.

1. Introduction

Significant damage to the environment is being inflicted by rapid industrialization and urbanization. This has resulted in the release of large amounts of harmful chemicals, gases and substances. Therefore, it is essential to understand the inherent properties of these products, and how they enhance the process of synthesizing nanoparticles. Biological molecules are especially suited for application in nanotechnology due to their special properties. The biological molecules are assembled into highly controlled assemblies to produce the metal nanoparticles, providing a reliable and environmentally friendly method [1]. Metal and semiconductor nanoparticle synthesis is a significant area of research due to its numerous applications in new technologies. Nanotechnology is a rapidly evolving field of study within current materials science. Nanoparticles possess completely new, or enhanced, characteristics; e.g., size, dispersion and particle shape. As a result, new and exciting uses for nanoparticles and nanomaterials are beginning to appear in many areas of study [2]. Most of the chemical processes used to manufacture nanoparticles are too expensive, contain toxic and dangerous chemicals and create serious biological hazards. These findings support the growing need for developing environmentally safe synthesis methods using "green" synthesis and biological alternatives [3]. Synthesis of nanoparticles using a variety of plants and their extracts may provide more advantages than other biological synthesis methods that utilize complex systems to maintain microorganisms in culture. In recent years, silver nanoparticles have been synthesized from natural sources (i.e., neem [4], legume plants [5], various leaf broths [6] and natural rubber [7]). Echinops spinosissimus is a rich source of phenolics and flavonoids with potent antioxidant, anti-inflammatory, and antimicrobial properties, making it an ideal and biocompatible reducing agent for the green synthesis of stable AgNPs with potential biomedical applications. Silver nanoparticles adhere to the cell wall of microorganisms, disrupting its permeability and cellular respiration. may infiltrate the cell wall, resulting in cellular damage through interactions with phosphorus- and sulfur -containing substances, such as DNA and proteins, within the cell [8]. The antibacterial activity of silver nanoparticles results from silver ion release, which is size-dependent—smaller particles show stronger effects. Biogenic

synthesis using microorganisms, such as bacteria and fungi, enhances nanoparticle biocompatibility for therapeutic use.

Making AgNPs from plants is a simple process where silver nitrate ($AgNO_3$) reacts with the natural compounds found in plant extracts. Nanoparticles are typically created through three phases: an ion reduction process initiates cluster formation ,reducing groups in the extract (–OH phenolic, –CHO, –SH, $–NH_2$) donate electrons to Ag^+, forming metallic Ag^0, which then promotes the growth of nanoparticles. As a result of the characteristics of each step of the reaction, there are many factors such as the type of reducing agent used, the concentration of the reducing agent, the amount of $AgNO^3$ and the pH level of the solution that affect how the reducing agent reduces Ag^+ ions to Ag^0. The hydroxyl (OH) groups of plant derived biomolecules like amino acids, proteins, alkaloids, flavonoids, polyphenols, enzymes, tannins, carbohydrates and saponins provide sites for the binding and stabilization of Ag^+ ions leading to the reduction of the Ag^+ ions to form Ag^0 [9] and ultimately the formation of AgNPs. The peel extract of P granatum contains kaempferol, flavanone naringin, and glycosides; all of these contain OH groups that can be used to reduce Ag^+ ions to AgNPs [10]. Based on the proposed mechanism for the synthesis of AgNPs using Tulsi leaf extract, quercetin found in Tulsi leaves reacts with Ag^+ ions to form a compound where the hydroxyl group is bonded to a carbon atom of an aromatic ring and thereby reducing Ag^+ to AgNPs and preventing aggregation [11]. The mechanism(s) involved in the stabilization of Ag^+ ions and reduction of the ions to AgNPs by phytochemicals has been little explored in this area and therefore, the mechanisms may vary by facility [12]. Therefore, it is necessary to conduct further research to identify the biomolecular capping/stabilizing agents in the synthesis of AgNPs from plants [13].

Hemolysis is the process by which erythrocytes (red blood cells) are broken down, releasing their components such as hemoglobin into the surrounding fluid environment. Hemolysis may lead to the development of anemia, jaundice, and renal failure [14] and RBC deformability and aggregation directly influence blood viscosity and therefore the function of microcirculation [15]. When blood flows normally through the body it delivers adequate oxygen, efficiently transports nutrients to tissues, and maintains steady metabolic processes. Minor changes in the deformability and aggregation of RBCs may lead to circulatory diseases within both macro- and microvascular systems [16]. The mechanical stability of RBC membranes is a reliable indicator for assessing in vitro cytotoxicity, particularly in the presence of cytotoxic compounds. Lyses can lead to various health effects and numerous disorders [17]. Microbial activity causes hemolysis in transferable diseases. Phenolic compounds, such as flavanols and glycosides, have a wide range of biological activities that are important for their antioxidant and cell-killing functions. Nanostructures can disrupt the RBC lipid bilayer, leading to hemolysis, along with electrostatic attraction associated with hemagglutination [18]. Researchers have demonstrated that the effects vary depending on the protein content of the blood. AgNPs are extensively used for their antimicrobial properties and as drug carriers in biomedical applications [19]. However, toxicological data regarding their effects on RBCs and the underlying mechanisms are still limited. The direct interaction of nanoparticles with red blood cells causes the cytotoxicity induced by AgNPs, leading to oxidative stress, membrane damage, and ultimately, hemolysis.

Hemolysis resulted from the release of oxidative stress products due to nanoparticle interactions with erythrocytes. Hemolysis was measured using spectroscopy methods over a range of silver nanoparticle concentrations [20, 21]. Since interactions between silver nanoparticles and blood components specifically erythrocytes will determine the toxicological effects of silver nanoparticles, this topic is important to understand the harmfulness of this toxic

substance. It is well known that the interaction of silver nanoparticles with proteins/peptides or other biomolecules depends on several features of the nanoparticles themselves; i.e., surface chemistry, stability, etc. In addition, it is now widely accepted that the toxicology of NPs is based upon their physical structure, chemical composition, material characteristics, binding affinity to biological sites and cellular uptake/excretion processes. As Shah (2018) indicated, the water extracts of Daphne mucronata leaves and their nanostructures did not have any cytotoxicity towards erythrocytes [22]. Based on this, the water extract of Daphne mucronata leaves and its AgNP's can be used safely for biological cells when present in small quantities. Similarly, Mohammed et al. (2019) reported that the aqueous leaf extract of C. lancifolius had an erythrocyte lysis rate of only 1.72% for healthy, non-smoking humans [15].

The primary purpose of this research project is to develop and describe eco-acceptable silver nanoparticles synthesized through the use of E. spinosissimus seed extract as well as to investigate their biological characteristics. This study will be used to find optimal environmental conditions for the production of AgNPs and will then analyze the properties of those produced particles with the aid of modern analytical methods (e.g., FTIR, SEM, XRD, and UV–Vis Spectroscopy) in order to assess their ability to inhibit the growth of various types of microorganisms that are of medical significance (bacteria and fungi). Additionally, the hemolysis produced by the AgNP's to red blood cells was evaluated so that the biocompatibility and possible cytotoxic effects of these NPs could be determined which would provide an overall evaluation of their biomedical applications and safety profiles.

2. **Experimental**

Materials: Echinops spinosissimus was collected from Iraq-Baghdad. Fisher Chemical AgNO3, a 99% pure analytical reagent grade, along with distilled water was added. Sigma Chemical Company provided acetic acid CH_3COOH with a purity of 90%, along with sodium bicarbonate ($NaHCO_3$).

Instrumentation: The produced nanoparticles were characterized using x-ray diffraction (XRD, XD-3, Persee, China), scanning electron microscopy (SEM, tescan-MIRA3, USA), atomic force microscopy (AFM, Nanosurf AG, Switzerland), Fourier transform infrared (FTIR, SHIMADZU 8400S, Japan), and UV-visible spectroscopy. (UV-vis. SHEMADZU 2601, Japan). GC-MS analysis was performed using the GCMS-QP2010 PLUS apparatus.

preparation of silver nitrate: A 0.1, 0.01, and 0.001 M silver nitrate stock solution was prepared by dissolving 3.4, 0.34, and 0.034 g of silver nitrate, respectively, in 200 ml of distillation water. Store the stock solutions in the dark until use.

preparation of plant extract: As shown in (FIGURE 1), E. spinosissimus plant seeds were dried to a consistent weight at 18°C in a confined, air-conditioned research lab. We ground the dried plant into a powder and dissolving 5 g in 100 ml of distillation water to improve the surface area for extraction, in which grinding the seeds into a fine powder reduces the particle size of the plant material, thereby increasing the total surface area exposed to the solvent (water) during extraction. The solution was heated to 100°C for 15 minutes and then filtered [5].

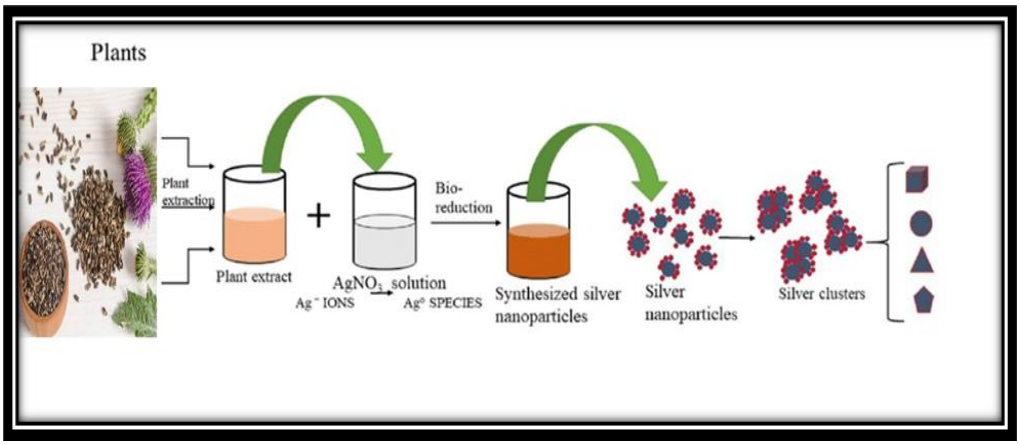


Figure 1: Schematic diagram for Ag-NP synthesis using Echinops spinosissimus extract

3. Results and Discussion

3.1. Optimized conditions for the green synthesis of AgNPs:

This section examines the effects of several parameters, including extract and $AgNO_3$ concentrations, temperature, pH, and incubation period [23].

3.1.1. Plant extract and AgNO3 concentrations

The objective of this research was to examine how varying the concentration of E. spinosissimus extracts and $AgNO_3$ solutions would affect the creation and stability of AgNPs. An increase in absorbance intensity occurred in direct proportion to the amount of E. spinosissimus extracts added into the reaction mixture, which indicated a higher rate of reduction of Ag^+ ions [24]. At higher amounts of E. spinosissimus extracts and $AgNO_3$ concentrations, the bioactive compounds present within the E. spinosissimus extract acted as a reducing agent for the silver and also provided stabilization of the nanoparticles thereby preventing them from aggregating. The best synthesis conditions were obtained when the volume of E. spinosissimus extracts was 10 mL, and the concentration of $AgNO_3$ solution was 10 mL of 0.02 M $AgNO_3$ solution.

3.1.2. Incubation time

The effects of incubation time on the synthesis of nanoparticles were studied through the changes in color and UV-Visible absorption spectrometry for 15, 30, 60, and 90 minutes. The rate of the increase in UV-Vis absorption increased as the incubation time was extended, which is consistent with the increasing concentration of formed silver nanoparticles (AgNPs). The solution that contained the silver nanoparticles showed an observable color change from pale yellow to dark brown, showing evidence of the formation of AgNPs [25].

3.1.3. Temperature

The influence of the reaction temperature on the synthesis process was examined by performing the reduction reaction at 30 °C, 50 °C, and 70 °C. Increasing the temperature accelerated the conversion of Ag^+ to Ag^0 and produced smaller, more uniform nanoparticles. The most favorable morphology and stability were obtained at 70 °C [26].

3.1.4. pH:

The pH of the reaction mixture was evaluated by adjusting it within a pH range of 5 – 9 to investigate how it would affect the formation of nanoparticles. In neutral to slightly alkaline environments (pH 7-8), the most effective AgNP reduction and stabilization occurred,

producing AgNPs of ideal size and distribution. Thus, pH 7 was determined to be an appropriate pH to use as the standard experimental condition for further studies [27].

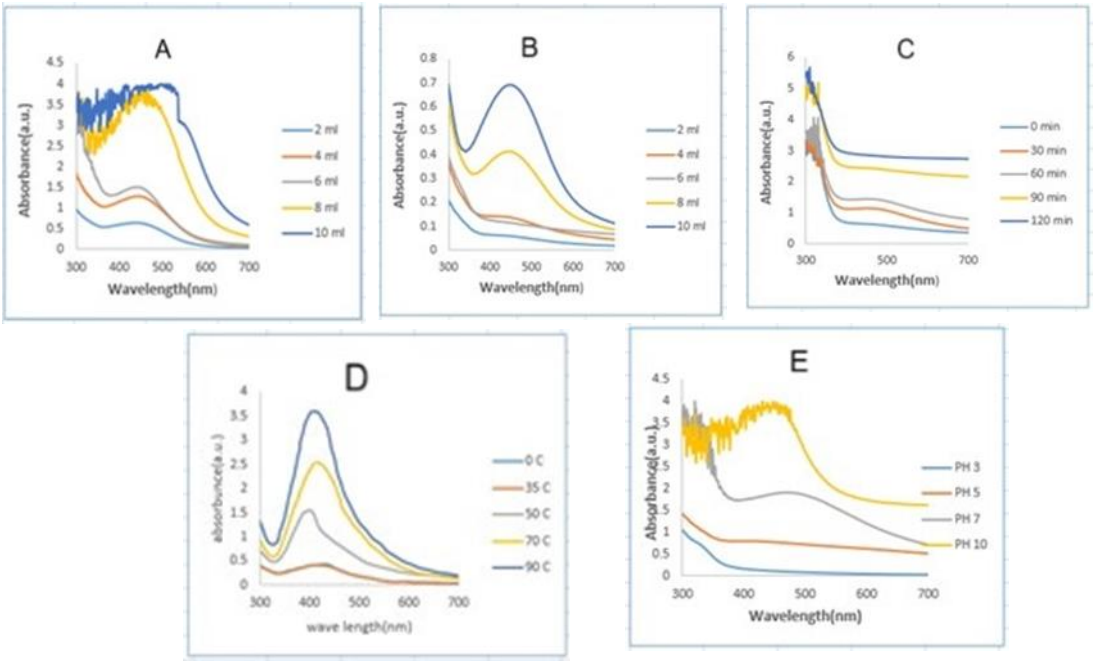


Figure 2:UV–visible spectrum for artificially produced silver nanoparticles: (a) E. spinosissimus at different volumes of $AgNO_3$; (b) $AgNO_3$ at different volumes of E. spinosissimus; (c) E. spinosissimus at different times; (d) E. spinosissimus at different temperatures; (e) E. spinosissimus at different pH of the reaction mixture.

Figure 2 shows the UV–visible absorption spectra of silver nanoparticles synthesized using Echinops spinosissimus extract under different reaction parameters: (A) Varying the volume of $AgNO_3$ revealed a direct relationship between the precursor concentration and absorbance intensity, where higher $AgNO_3$ volumes produced stronger surface plasmon resonance (SPR) peaks, indicating greater nanoparticle formation. (B) Increasing the volume of plant extract also enhanced absorbance, suggesting that a larger amount of phytochemicals was available to reduce Ag^+ ions and stabilize the resulting nanoparticles. (C) The effect of incubation time showed that the absorbance progressively increased with the reaction duration, accompanied by a color transition from light yellow to deep brown, confirming the gradual formation and accumulation of AgNPs. (D) Temperature variation demonstrated that higher temperatures (up to 70 °C) accelerated the reduction of silver ions, yielding more intense and sharper SPR peaks corresponding to smaller and more uniform nanoparticles, whereas excessive heating (90 °C) slightly decreased the stability. (E) The influence of pH indicated that near-neutral to mildly basic conditions (pH 7–8) favored the highest absorbance, reflecting optimal reduction and stabilization efficiency. Acidic or highly alkaline media led to broader or weaker peaks, indicating irregular particle growth or aggregation. Overall, these spectra confirm that the synthesis of AgNPs is strongly dependent on $AgNO_3$ concentration, extract volume, incubation time, temperature, and pH, with optimal conditions obtained at 10 mL extract, 10 mL of 0.02 M $AgNO_3$, pH 7, and 70 °C.

3.2. Characterization of the AgNPs

Before using synthesized AgNPs, specific methods must be employed to confirm the successful synthesis of the particles. The primary method for verifying the formation of AgNPs is through visual observation of the solution's color transition from a yellow color to a brown

color. The spectrophotometer is then used to verify the previous tracking method and to identify peaks of the nanoparticles in the visible range of the UV-VIS spectrum from approximately 400 to 450 nm. SEM and EDX are additional tools that can provide insight into the size, morphology, distribution, and chemical composition of the nanoparticles. The formation of nanoparticles may also be evaluated by means of X-ray diffraction (XRD). In addition to identifying nanoparticle formation, FTIR spectroscopy may be used to monitor the influence of biomolecules on both the production and stability of the nanoparticles.

3.2.1. **SEM**

As shown in Figures 3 (a) and (b), the particle size ranges from 19.49 to 23.4 nm, with sporadic agglomerations. The bio-organic capping molecules and plant extract may have formed hydrogen bonds and electrostatic interactions, resulting in these spherical forms. The presence of pure Ag nanoparticles was also verified by energy-dispersive X-ray spectroscopy (EDX). Figure 3(b) illustrates the elemental composition of Ag nanoparticles, showing significant signals for Ag (12.81%) and a minor proportion of carbon (31.76%), oxygen (41.88%), and chloride (2.22%) components. These components are attributed to the varying abundance and composition of the capping agents present in the extract. According to figures (3.b.), the particles have a spherical form with a particle size range of 19.49–54.57 nm, with some agglomerations, as shown in Figure (3.b).

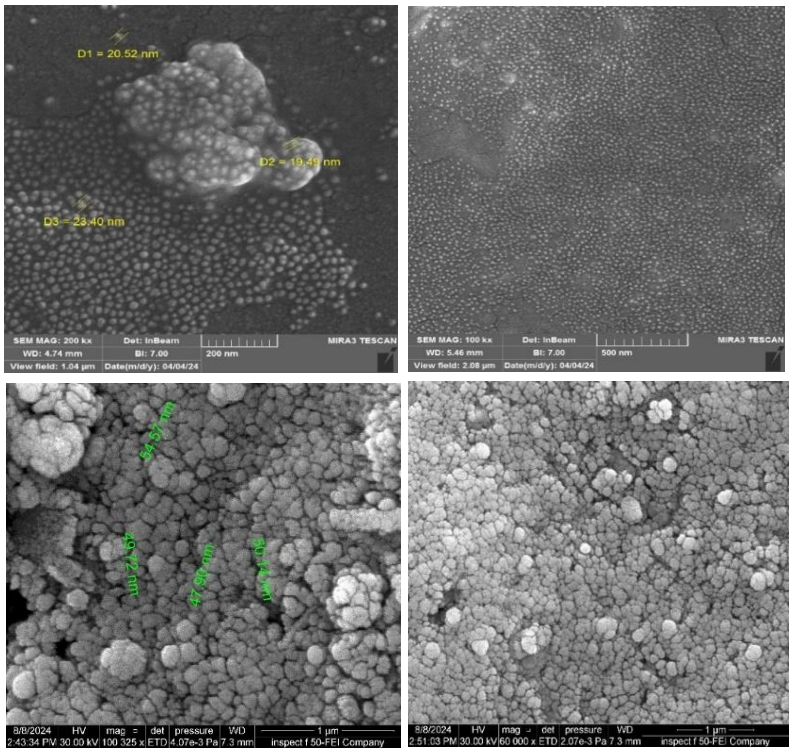
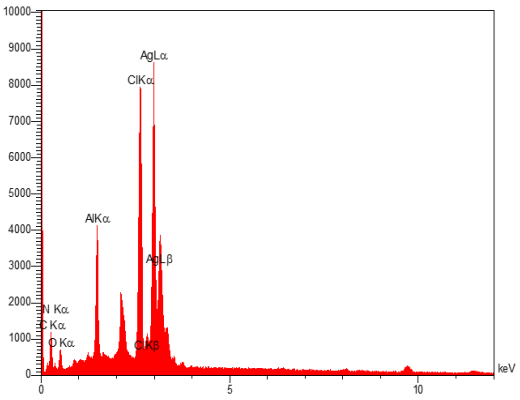


Figure 3: a. SEM analysis of the spherical shape of artificially produced silver nanoparticles at 200 ko.



Quantitative Results

Elt	Line	Int	Error	K	Kr	W%	A%
C	Ka	122.3	54.1027	0.0960	0.0566	14.29	31.76
N	Ka	33.7	54.1027	0.0267	0.0157	5.95	11.34
O	Ka	71.6	54.1027	0.0571	0.0336	25.09	41.88
Cl	Ka	51.1	56.4763	0.0463	0.0273	2.94	2.22
Ag	La	836.2	56.4763	0.7739	0.4558	51.74	12.81
				1.0000	0.5890	100.00	100.00

Figure 3: b. Energy-dispersive X-ray spectroscopy (EDX) of Ag NPs.

1.1.1. **Atomic Force Microscopy (AFM):** We used the atomic force microscope to investigate the surface morphology, mean particle size distribution, root mean square height (Sq), and surface roughness (Sa), which we calculated using SPIP Mountains software [28]. The three-dimensional images in Figure (4) show that the AgNPs in the 3D image appear spherical with a uniform distribution in the scanned area (3.58 x 3.58 m). The mean diameter of 843 particles in the desired area is 99.7 nm (Figure 4). We scanned the samples using the tapping mode, determining surface roughness by changing the height and representing it with parameters Sa (8.199 nm) and Sq (11.7 nm).

(a)

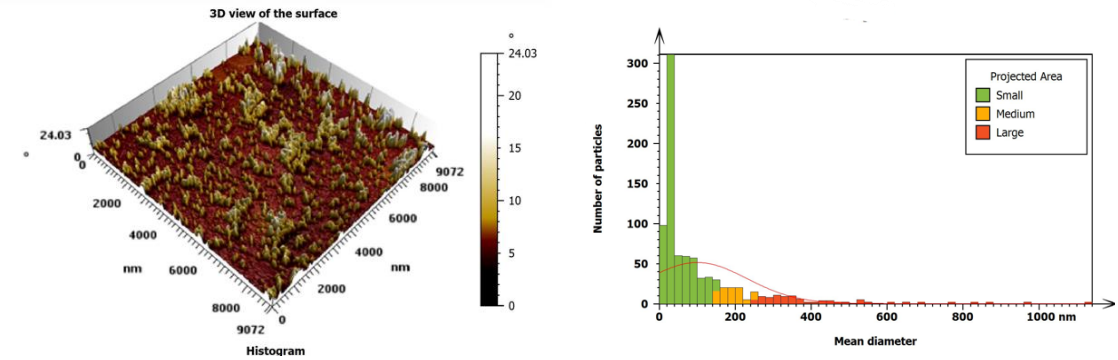


Figure 4: (a) AFM images of AgNPs made by green methods. (b) Distribution of nanoparticle diameter ranges

1.1.1. **FTIR spectroscopy of AgNPs:** The functional groups responsible for the effective stability and surface coating of the nanoparticles can be identified by comparing the FTIR spectra of the biosynthesized AgNPs with an extract from a medicinal plant. FTIR spectroscopy is a useful and inexpensive way to determine the role that biological molecules play in making green-generated AgNPs and maintaining their stability. Figure 5 displays the FTIR analysis of $AgNO_3$ and AgNPs using an Echinops spinosissimus extract in the range of 4000–400 cm^{-1}. The FTIR spectrum of AgNPs showed several absorption peaks at 3479, 3000, 1680, 1694, 1455, 1043, 882, 665, and 522 cm^{-1}. When the plant extract was added to the $AgNO_3$ solution, the absorption peaks in the FTIR spectrum changed. This showed that the amount of Ag(I) decreased and the plant extract helped to cap and stabilize the NPs that were made. The large absorption peak at 3479.58 cm^{-1} is caused by the polyphenolic components of Echinops spinosissimus extract. This peak is related to the O-H stretching of the free hydroxyl group. The absorption peak at 1649.14 cm^{-1} indicated the presence of C=O stretching in carboxylic acids or aromatic compounds, the peak at 1680 cm^{-1} indicated C=C stretching of alkenes, the peak at

1455.26 cm^{-1} indicated C-C aromatics, the peak at 1043 cm^{-1} indicated O-H bending for carboxylic acid, alcohol, and C-O stretching, and the small bands at 822 cm^{-1} correlated with the metal-oxygen stretching vibrations.

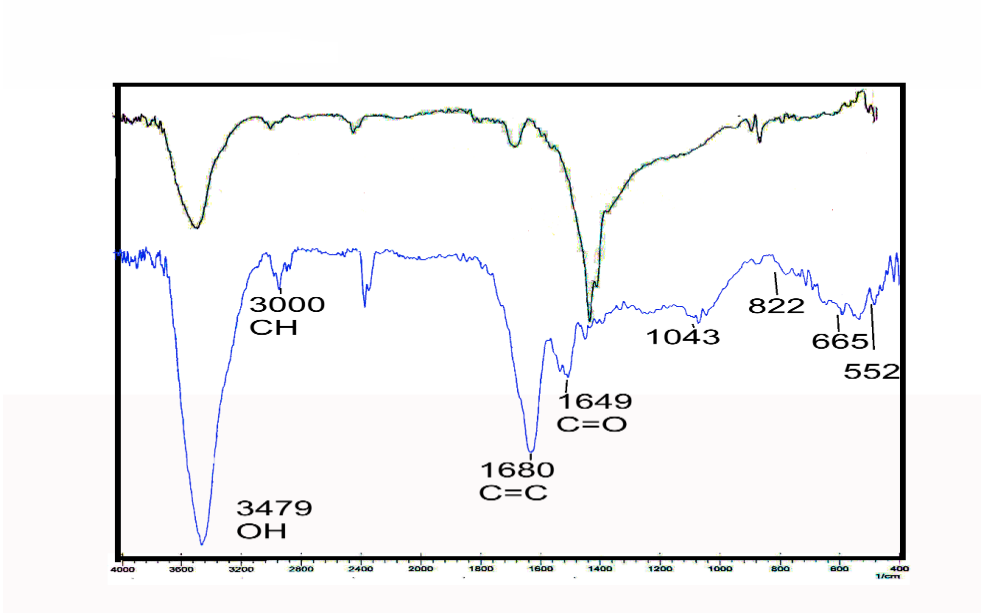
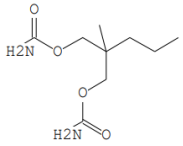
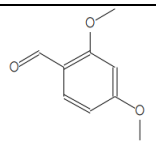
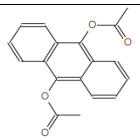
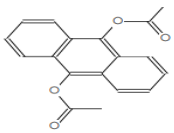
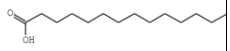
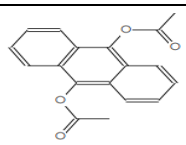
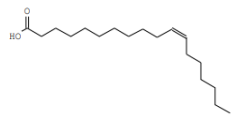
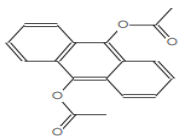
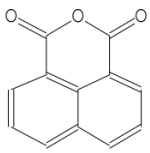
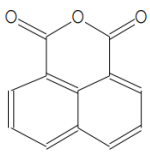
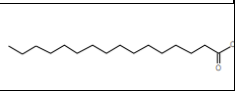
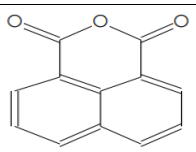
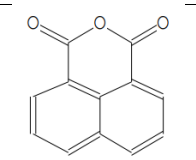
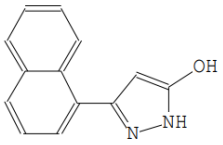
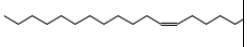
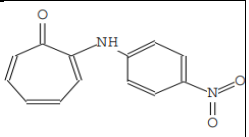
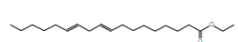
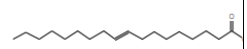
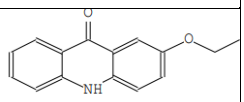
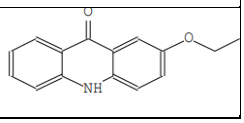


Figure 5: Fourier transform infrared spectra of AgNPs (a) $AgNO_3$ (b) AgNPs with Echinops spinosissimus extract

1.1.1. Gas chromatography-mass spectrometry (GC-MS) analysis: The inert column is made up of fused silica capillary columns that are joined together with dimethylpolysiloxane. It is not polar. It shares a close relationship with mass spectroscopy. Helium was used as the carrier gas, and it was pumped through a 30-m-long column at a speed of 30 ml/min. We established a temperature of 250 °C for the injector port. We adjusted the oven's temperature to start at a steady 30°C for 3 min, rise to 200°C at a rate of 3°C per min, and stay at an isothermal 200°C for 15 min. A 2-microliter volume of a 0.2% ethanol-dissolved solution was added to the mixture at 280°C. There was a 2:1 split ratio. The ionization voltage was 72 electron volts. The ion source temperature is 280 °C. The proportionate amount of each ingredient was determined by comparing its average peak area to the total areas. We operated the equipment and collected data using the supplied mass spectroscopy solution software [29]. The primary methods for identifying phytochemicals are analyzing their peak area, molecular weight, retention time, and molecular formula. Table 2 lists the 20 compounds identified in the GC fractions of the E. spinosissimus ethanolic extract. By acting as reducing agents, it also functions as a capping agent, enhancing the stability of AgNPs and boosting their usefulness in biological applications.

Table 1: GC-MS spectral analysis of the ethanoic extract of Echinops spinosissimus respectively:

NO.	Retention time (min)	Name of compound	Molecular formula	Molecular weight	Peak area (%)	Chemical structures
1	9.975	Meprobamate	$C_9H_{18}N_2O_4$	218	0.99	
2	10.054	Benzaldehyde, 2,4-dimethoxy-	$C_9H_{10}O_3$	166	1.65	
3	11.436	9,10-Anthracenediol	$C_{18}H_{14}O_4$	294	5.42	
4	11.469	9,10-Anthracenediol,	$C_{18}H_{14}O_4$	294	9.33	
5	11.555	Pentadecanoic acid	$C_{15}H_{30}O_2$	242	0.56	
6	11.986	9,10-Anthracenediol	$C_{18}H_{14}O_4$	294	2.55	
7	12.400	cis-Vaccenic acid	$C_{18}H_{34}O_2$	282	0.51	
8	12.530	9,10-Anthracenediol	$C_{18}H_{14}O_4$	294	32.41	
9	12.708	Naphthalic anhydride	$C_{12}H_6O_3$	198	1.42	
10	12.949	9,10-Anthracenediol	$C_{18}H_{14}O_4$	294	30.43	
11	13.136	Hexadecanoic acid	$C_{18}H_{36}O_2$	284	1.31	

12	13.205	Naphthalic anhydride	$C_{12}H_6O_3$	198	0.68	
13	13.281	9,10-Anthracenediol	$C_{18}H_{14}O_4$	294	5.43	
14	13.325	5-Naphthalen-1-yl-2H-pyrazol-3-ol	$C_{13}H_{10}N_2O$	210	1.87	
15	13.975	6-Octadecenoic acid	$C_{18}H_{34}O_2$	282	0.99	
16	14.014	2-(p-Nitroanilino)tropone	$C_{13}H_{10}N_2O_3$	242	1.16	
17	14.154	9,12-Octadecadienoic acid	$C_{20}H_{36}O_2$	308	0.72	
18	14.209	9-Octadecenoic acid	$C_{20}H_{38}O_2$	310	0.79	
19	14.246	2-Ethoxy-10H-acridin-9-one	$C_{15}H_{13}NO_2$	239	1.21	
20	14.441	2-Ethoxy-10H-acridin-9-one	$C_{15}H_{13}NO_2$	239	0.57	

4. Application of AgNPs:

4.1. **Antibacterial activity of AgNPs: AgNPs** are widely used in medicine. AgNPs have an antagonistic effect on certain species of bacteria. In this study, we looked at how biologically synthesized silver nanoparticles, shown in Figure 6, worked against two types of harmful bacteria, Gram-positive and Gram-negative, using Echinops spinosissimus. Numerous studies have demonstrated that AgNPs affect bacteria by interacting with proteins that come into contact with sulfur, thereby damaging the bacteria's ability to breathe and causing them to become distracted [30]. AgNPs were excellent at killing Escherichia coli (a Gram-negative bacteria) and Staphylococcus aureus (a Gram-positive bacteria). This was true at different concentrations of AgNPs (100%, 75%, 50%, and 25%), as shown in Figure 6.

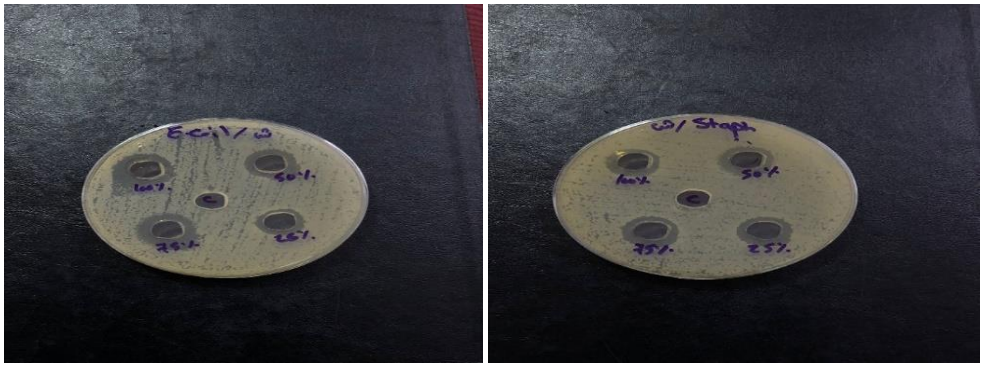


Figure 6: Antibacterial activity of silver nanoparticles using Echinops spinosissimus extract against Escherichia coli and Staphylococcus aureus.

The recorded diameters (in mm) of the inhibition zones of E. spinosissimus against E. coli surround the discs 17 mm, 18 mm, 15 mm, and 14 mm at higher concentrations (100%, 75%, 50%, 25%). The inhibition zones of Echinops spinosissimus against Staphylococcus aureus of recorded diameters (in mm) surrounding the discs 14 mm, 15 mm, 14 mm, and 15 mm at higher concentrations (100%, 75%, 50%, 25%). The effectiveness of Ag NPs at low concentrations (25%) was reduced in eliminating microorganisms. The antibacterial activity of the biosynthesized AgNPs is consistent with a multifactorial mechanism in which surface oxidation releases Ag^+ that interacts with membrane thiol-containing enzymes, disrupts permeability, and promotes reactive-oxygen-species generation, collectively impairing DNA, proteins, and energy metabolism. These processes align with the inhibition-zone data: E. coli exhibited a clear dose dependence, with larger zones at higher nanoparticle concentrations and attenuation at 25%, indicating greater sensitivity to Ag^+ availability and particle–membrane contact in gram-negative cells. In contrast, S. aureus showed relatively stable inhibition across concentrations, a pattern compatible with the thicker peptidoglycan barrier of gram-positive cells that narrows the dynamic response [31].

4.2. **Antifungal activity of Ag nanoparticles:** The antifungal activity of Ag nanoparticles is one of its well-known broad-spectrum antibacterial characteristics [30]. several processes, including breaking down cell membranes and producing dangerous silver ions and reactive oxygen species, make silver nanoparticles very effective at killing fungi. However, for safe and efficient usage, careful consideration of their size, concentration, and potential toxicity is essential.

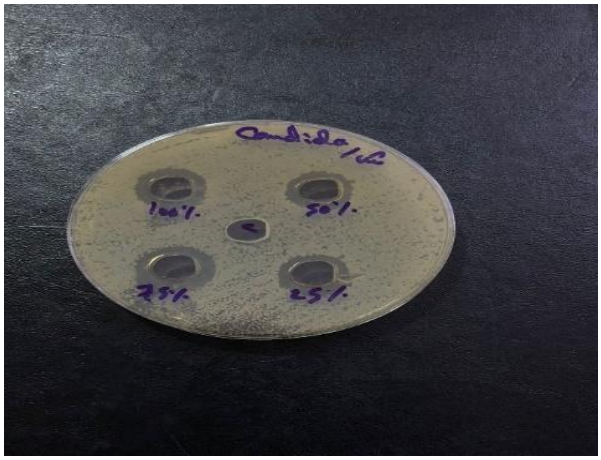


Figure 7: Antifungal activity of AgNPs utilizing the plant extract Echinops spinosissimus against Candida**.**

The inhibition zones of Ag nanoparticles against Candida, the largest genus of yeasts with therapeutic significance and the most common cause of fungal diseases globally, have recorded diameters (in mm) surrounding the discs, as shown in Figure (7). These diameters are 15, 18, 15, and 15 mm at concentrations of 100%, 75%, 50%, and 25%, respectively.

Table 2: Recorded diameters for antifungal and antibacterial activity of Ag NPs in relation to Ag NPs concentrations and bacterial isolates of E. spinosissimus

Concentrations of Ag NPs / Bacterial Isolates	100%	75%	50%	25%
Escherichia coli	17	18	15	14
Staphylococci aureus	14	15	14	15
Candida	15	18	15	15

4.3. Hemolytic Activity

Numerous nanoparticles are recognized for their ability to induce considerable cytotoxicity and elicit an oxidative stress response in diverse cell types. AgNPs are considered among the most dangerous NPs due to their metallic silver content and elevated biological reactivity. The effects and mechanisms of toxicity have been thoroughly examined in various cell lines and animal models. Nonetheless, an uncommon investigation that elucidates the harmful effects and mechanisms of AgNP exposure on RBCs has been undertaken in this domain. As the injection of AgNP-based therapy into the vascular system increases, direct interactions between AgNPs and erythrocytes are likely to occur more frequently. This study examined the adsorption, absorption, and hemolytic potentials of AgNPs of various sizes in RBCs [32].

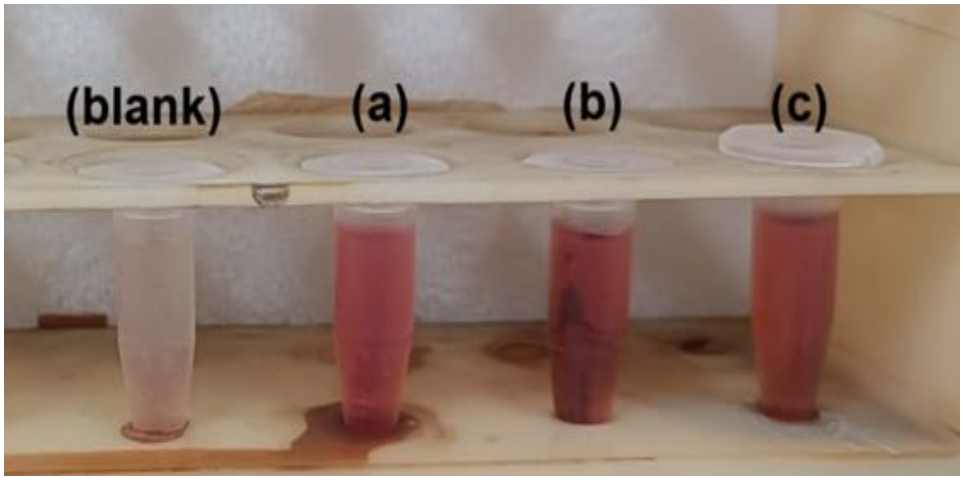


Figure 8. Red blood cells exposed to silver nanoparticles at different concentrations.

The peaks of the spectra in FIGURE 9, due to localized surface plasmon resonance of AgNPs, have an absorption maximum around ~400 nm (with a bandwidth of approximately ±5 nm) and increase with an increasing amount of AgNPs; the absorbance of AgNPs measured from the peak heights is about ~0.11 at 0% AgNP, ~0.18 at 20% AgNP, ~0.22 at 50% AgNP, and ~0.27 at 80% AgNP. Therefore, our measurements indicate that there is a larger number of formed AgNPs and consequently a higher optical density with increasing concentration of AgNPs. In addition, we found that the influence of AgNP-exposure on cells, i.e., oxidative stress and hemolysis, depends strongly on the concentration of the AgNP. Besides the size, shape, and coating of the nanoparticles, another major parameter determining the toxicity and

absorption capability of nanoparticles is their concentration when they come into contact with red blood cells (RBC). For example, as shown in a quantitative study, the absorption of polystyrene nanoparticles by RBC increases with concentration [33]. Only significant uptake was observed at high enough concentrations, so that concentration appears to be important for the RBC internalization of nanoparticles. Recent studies concerning gold nanoparticles [34] TiO_2 nanoparticles [35] and hydroxyapatite nanoparticles [36] also demonstrate that higher amounts of these types of nanoparticles will generally cause greater damage to RBCs than lower amounts of nanoparticles. Nonetheless, some other studies reported that increasing the concentration of nanoparticles leads to decreasing hemolytic activity for some types of nanoparticles (e.g., fumed silica [36], mesoporous silica [36], and colloidal amorphous silica [36]). This indicates that both the type and concentration of NPs can interact in a complex manner with each other to produce hemolytic effects.

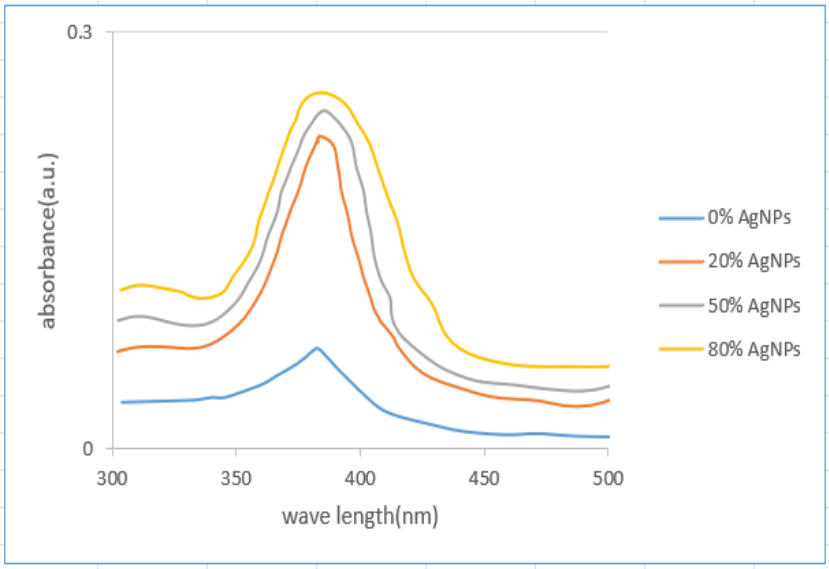


Figure 9: The UV–visible spectrum for different concentrations of silver nanoparticles shows the difference in the hemolysis rate of RBCs with increasing concentration**.**

The mechanism through which AgNPs may cause hemolysis in erythrocytes remains unclear. The mechanism by which AgNPs cause hemolysis in erythrocytes is unclear. It is unclear how AgNPs cause hemolysis, as it is not known if it happens because the particles directly interact with the cells, because free silver ions are released, or a combination of both. The lack of major hemolytic effects from silver ions in this study suggests that the direct contact of AgNPs with red blood cells (RBCs) is the main cause of hemolysis (Fig. 10). AgNPs are known to attach with great affinity to thiol groups in biological entities, such as proteins or membrane phospholipids, thereby facilitating their denaturation. The negatively charged Ag surface will significantly interact with the organic cations in the RBC membrane, thereby contributing to hemolysis. Therefore, we hypothesized that the increased reactivity and better movement of small AgNPs, compared to larger particles, might lead to more [37].

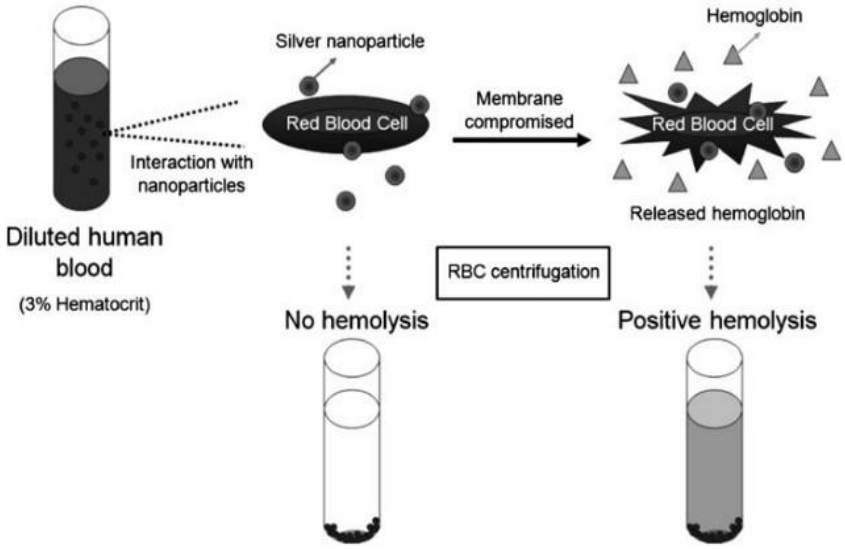


Figure 10: In vitro hemolysis of silver nanoparticles in human blood

Conclusion

This paper describes the successful green synthesis of silver nanoparticles (AgNPs) utilizing Echinops spinosissimus seed extract, which provides an environmentally benign and efficient method of nanoparticle production. FTIR, SEM, AFM and UV-vis analysis showed the generation of AgNPs. The best synthesis conditions were 10 mL of extract and silver nitrate solution (2×10^{-2} M) at pH 7, 70 °C, and 1 h reaction duration. The SEM analysis revealed that the particles were mostly round and rod-shaped, measuring 46.69–71.99 nm in size. The biosynthesized AgNPs showed strong antibacterial effects against E. coli, Klebsiella, and Staphylococcus aureus, with areas of inhibition ranging from 14 to 18 mm. AgNPs were found to exhibit strong fungicidal activity against Candida species (with zone of inhibitions ranging from 15-18 mm). However, cytotoxic effects were observed through a concentration dependent manner in a hemolytic assay which indicates that dosage is an important consideration prior to application of these materials in biomedicine. The Echinops spinosissimus plant can be used as a cost effective means to produce antimicrobial AgNPs. Additional research needs to include in vivo testing along with mechanisms of action of hemolysis to evaluate whether these products are safe and have therapeutic value for clinical use. In general, AgNPs produced by Echinops spinosissimus possess high antibacterial activity; however, it will be necessary to investigate the safety of these products in medicine at various doses.

References

[1] Y. Khan et al., "Classification, synthetic, and characterization approaches to nanoparticles, and their applications in various fields of nanotechnology: a review," *Catalysts*, vol. 12, no. 11, p. 1386, 2022, doi: 10.3390/catal12111386.

[2] S. Khan and M. K. Hossain, "Classification and properties of nanoparticles," *Nanoparticle-Based Polymer Composites*, Woodhead Publishing, pp. 15–54, 2022.

[3] T. A. Saleh, "Trends in nanomaterial types, synthesis methods, properties and uses: Toxicity, environmental concerns and economic viability," *Nano-Structures & Nano-Objects*, vol. 37, p. 101109, 2024, doi: 10.1016/j.nanoso.2024.101109.

[4] S. K. Moorthy, C. H. Ashok, K. V. Rao, and C. Viswanathan, "Synthesis and characterization of MgO nanoparticles by neem leaves through green method," *Materials Today: Proceedings*, vol. 2, no. 9, pp. 4360–4368, 2015, doi: 10.1016/j.matpr.2015.10.027.

[5] R. Kumari, J. S. Singh, and D. P. Singh, "Biogenic synthesis and spatial distribution of silver nanoparticles in the legume mungbean plant (Vigna radiata L.)," *Plant Physiology and Biochemistry*, vol. 110, pp. 158–166, 2017, doi: 10.1016/j.plaphy.2016.06.001.

[6] S. L. Smitha, D. Philip, and K. G. Gopchandran, "Green synthesis of gold nanoparticles using Cinnamomum zeylanicum leaf broth," *Spectrochimica Acta Part A: Molecular and Biomolecular Spectroscopy*, vol. 74, no. 3, pp. 735–739, 2009, doi: 10.1016/j.saa.2009.08.007.

[7] N. A. Bakar, J. Ismail, and M. A. Bakar, "Synthesis and characterization of silver nanoparticles in natural rubber," *Materials Chemistry and Physics*, vol. 104, nos. 2–3, pp. 276–283, 2007, doi: 10.1016/j.matchemphys.2007.03.015.

[8] I. P. Sæbø, M. Bjørås, H. Franzyk, E. Helgesen, and J. A. Booth, "Optimization of the hemolysis assay for the assessment of cytotoxicity," *International Journal of Molecular Sciences*, vol. 24, no. 3, p. 2914, 2023, doi.org/10.3390/ijms24032914.

[9] S. Yadav, T. Nadar, J. Lakkakula, and N. S. Wagh, "Biogenic synthesis of nanomaterials: bioactive compounds as reducing, and capping agents," *Biogenic Nanomaterials for Environmental Sustainability: Principles, Practices, and Opportunities*, Cham: Springer International Publishing, 2024, pp. 147–188. doi, 10.1007/978-3-031-45956-6_7

[10] A. P. McNamee and M. J. Simmonds, "Red blood cell sublethal damage: hemocompatibility is not the absence of hemolysis," *Transfusion Medicine Reviews*, vol. 37, no. 2, p. 150723, 2023, doi: 10.1016/j.tmrv.2023.03.001

[11] O. K. Baskurt and H. J. Meiselman, "Blood rheology and hemodynamics," in *Seminars in Thrombosis and Hemostasis*, vol. 50, no. 6, pp. 902–915, 2024 , doi: 10.1055/s-0043-1777802

[12] L. M. Al Masoudi and A. M. Hashim, "Morphological features and biological activity of different extracts of Echinops spinosissimus grown in Saudi Arabia," *Agronomy*, vol. 13, no. 2, p. 573, 2023, doi: 10.3390/agronomy13020573.

[13] H. M. Abuzeid, C. M. Julien, L. Zhu, and A. M. Hashem, "Green synthesis of nanoparticles and their energy storage, environmental, and biomedical applications," *Crystals*, vol. 13, no. 11, p. 1576, 2023, doi.org/10.3390/cryst13111576.

[14] A. Naganthran et al., "Synthesis, characterization and biomedical application of silver nanoparticles," *Materials*, vol. 15, no. 2, p. 427, 2022 , doi: 10.3390/ma15020427

[15] N. Liaqat, N. Jahan, T. Anwar, and H. Qureshi, "Green synthesized silver nanoparticles: Optimization, characterization, antimicrobial activity, and cytotoxicity study by hemolysis assay," *Frontiers in Chemistry*, vol. 10, p. 952006, 2022, doi.org/10.3389/fchem.2022.952006.

[16] F. Hao and X.-P. Yan, "Nano-sized zeolite-like metal-organic frameworks induced hematological effects on red blood cells," *Journal of Hazardous Materials*, vol. 424, p. 127353, 2022, doi: 10.1016/j.jhazmat.2021.127353.

[17] E. Elatafi and J. Fang, "Effect of silver nitrate (AgNO3) and nano-silver (Ag-NPs) on physiological characteristics of grapes and quality during storage period," *Horticulturae*, vol. 8, no. 5, p. 419, 2022 , doi: 10.3390/horticulturae8050419.

[18] W. W. Melkamu and L. T. Bitew, "Green synthesis of silver nanoparticles using Hagenia abyssinica (Bruce) J. F. Gmel plant leaf extract and their antibacterial and antioxidant activities," *Heliyon*, vol. 7, no. 11, e08459, 2021, doi: 10.1016/j.heliyon.2021.e08459.

[19] M. Ansari et al., "Plant mediated fabrication of silver nanoparticles, process optimization, and impact on tomato plant," *Scientific Reports*, vol. 13, no. 1, p. 18048, 2023 , doi: 10.1038/s41598-023-45038-x

[20] H. Liu, H. Zhang, J. Wang, and J. Wei, "Effect of temperature on the size of biosynthesized silver nanoparticle: deep insight into microscopic kinetics analysis," *Arabian Journal of Chemistry*, vol. 13, no. 1, pp. 1011–1019, 2020 , doi: 10.1016/j.arabjc.2017.09.004

[21] S. S. Birla, S. C. Gaikwad, A. K. Gade, and M. K. Rai, "Rapid synthesis of silver nanoparticles from Fusarium oxysporum by optimizing physicocultural conditions," *The Scientific World Journal*, vol. 2013, no. 1, p. 796018, 2013 , doi: 10.1155/2013/796018

[22] M. A. Hussain and W. N. Al Sieadi, "Determination and removal of methylene blue dye via photodegradation using titanium dioxide nanoparticles from watermelon rind," *Al-Mustansiriyah Journal of Science*, vol. 8, no. 1, no. 362, 2025, doi: 10.24200/amecj.v8.i01.362.

[23] H. Ibrahim, A. J. Uttu, M. S. Sallau, and O. R. A. Iyun, "Gas chromatography–mass spectrometry (GC–MS) analysis of ethyl acetate root bark extract of Strychnos innocua (Delile)," *Beni-Suef*

University Journal of Basic and Applied Sciences, vol. 10, no. 1, p. 65, 2021, doi: 10.1186/s43088-021-00156-1.

[24] P. Nie, Y. Zhao, and H. Xu, "Synthesis, applications, toxicity and toxicity mechanisms of silver nanoparticles: A review," *Ecotoxicology and Environmental Safety*, vol. 253, p. 114636, 2023, doi: 10.1016/j.ecoenv.2023.114636.

[25] A. M. Carpenter and M. L. van Hoek, "Development of a defibrinated human blood hemolysis assay for rapid testing of hemolytic activity compared to computational prediction," *Journal of Immunological Methods*, vol. 529, p. 113670, 2024, doi.org/10.1016/j.jim.2024.113670.

[26] S. Yadav, S. Bhagat, S. Singh, and P. K. Maurya, "Comparative study of antioxidant activity of dextran-coated iron oxide, gold, and silver nanoparticles against age-induced oxidative stress in erythrocytes," *The Journals of Gerontology, Series A: Biological Sciences and Medical Sciences*, vol. 79, no. 11, p. glae197, 2024, doi: 10.1093/gerona/glac197.

[27] A. V. Aseichev, O. A. Azizova, E. M. Beckman, O. I. Skotnikova, L. B. Dudnik, O. N. Shcheglovitova, and V. I. Sergienko, "Effects of gold nanoparticles on erythrocyte hemolysis," *Bulletin of Experimental Biology and Medicine*, vol. 156, no. 4, pp. 495–498, 2014 , doi: 10.1007/s10517-014-2383-6

[28] M. Ghosh, A. Chakraborty, and A. Mukherjee, "Cytotoxic, genotoxic and the hemolytic effect of titanium dioxide (TiO_2) nanoparticles on human erythrocyte and lymphocyte cells in vitro," *J. Appl. Toxicol*., vol. 33, no. 10, pp. 1097–1110, 2013, doi.org/10.1002/jat.2863

[29] M. M. Masood and W. N. J. Al Sieadi, "Eco-Friendly synthesis of nickel oxide nanoparticles using licorice leaves extract for anticancer effect against bone cancer cells MG-63 and antibacterial activity," *Iraqi Journal of Science*, vol. 66, no. 9, pp. 3635–3654, Sep. 2025, doi: 10.24996/ijs.2025.66.9.12.

[30] M. Y. Elgendy et al., "Antibacterial activity of silver nanoparticles against antibiotic-resistant Aeromonas veronii infections in Nile Tilapia, Oreochromis niloticus (L.), in vitro and in vivo assay," *Aquaculture Research*, vol. 53, no. 3, pp. 901–920, 2022 , doi: 10.1111/are.15632

[31] E. O. Mikhailova, "Green silver nanoparticles: an antibacterial mechanism," *Antibiotics*, vol. 14, no. 1, no. 5, 2024 , doi: 10.3390/antibiotics14010005

[32] O. A. Ghareeb, R. R. Sulaiman, and S. H. Ibrahim, "Impact of silver nanoparticles on hematological profiles and hepatorenal functions in photosensitivity: In Vivo," *Annals of the Romanian Society for Cell Biology*, vol. 25, no. 4, pp. 7448–7459, 2021.

[33] W. Ahmad, S. C. Bhatt, M. Verma, V. Kumar, and H. Kim, "A review on current trends in the green synthesis of nickel oxide nanoparticles, characterizations, and their applications," *Environmental Nanotechnology, Monitoring & Management*, vol. 18, p. 100674, 2022, doi.org/10.1016/j.enmm.2022.100674.

[34] A. Meher, A. Tandi, S. Moharana, S. Chakroborty, S. S. Mohapatra, A. Mondal, and P. Chandra, "Silver nanoparticle for biomedical applications: A review," *Hybrid Advances*, vol. 6, p. 100184, 2024, doi: 10.1016/j.hybadv.2024.100184.

[35] M. Jangra, G. Saini, P. Sheoran, A. Gahlaut, and V. Raj, "Advances in silver nanoparticles: Synthesis, characterization, and diverse applications in medicine, environment, antimicrobial and antiviral research," *Critical Reviews in Analytical Chemistry*, pp. 1–25, 2025, doi: 10.1080/10408347.2025.2307398.

[36] M. S. Laranjeira et al., "Different hydroxyapatite magnetic nanoparticles for medical imaging: Its effects on hemostatic, hemolytic activity and cellular cytotoxicity," *Colloids and Surfaces B: Biointerfaces*, vol. 146, pp. 363–374, 2016 , doi: 10.1016/j.colsurfb.2016.06.042

[37] R. Luna-Vázquez-Gómez et al., "Hemolysis of human erythrocytes by Argovit™ AgNPs from healthy and diabetic donors: An in vitro study," *Materials*, vol. 14, no. 11, Art. no. 2792, 2021 , doi: 10.3390/ma14112792